Environmental Pollution 262 (2020) 114257

Contents lists available at ScienceDirect

Environmental Pollution

journal homepage: www.elsevier.com/locate/envpol

Investigation of the spatially varying relationships of $PM_{2.5}$ with meteorology, topography, and emissions over China in 2015 by using modified geographically weighted regression☆

Qianqian Yang [a], Qiangqiang Yuan [a, b, *], Linwei Yue [c], Tongwen Li [d]

[a] School of Geodesy and Geomatics, Wuhan University, Wuhan, Hubei, 430079, China
[b] Key Laboratory of Geospace Environment and Geodesy, Ministry of Education, Wuhan University, Wuhan, 430079, Hubei, China
[c] School of Geography and Information Engineering, China University of Geosciences, Wuhan, Hubei, 430074, China
[d] School of Resource and Environmental Sciences, Wuhan University, Wuhan, Hubei, 430079, China

ARTICLE INFO

Article history:
Received 29 August 2019
Received in revised form
21 February 2020
Accepted 21 February 2020
Available online 28 February 2020

Keywords:
Fine particulate matter
Impacting factors
Relationship analysis
Spatial heterogeneity
Modified GWR

ABSTRACT

$PM_{2.5}$ pollution is caused by multiple factors and determining how these factors affect $PM_{2.5}$ pollution is important for haze control. In this study, we modified the geographically weighted regression (GWR) model and investigated the relationships between $PM_{2.5}$ and its influencing factors. Experiments covering 368 cities and 9 urban agglomerations were conducted in China in 2015 and more than 20 factors were considered. The modified GWR coefficients (MGCs) were calculated for six variables, including two emission factors (SO_2 and NO_2 concentrations), two meteorological factors (relative humidity and lifted index), and two topographical factors (woodland percentage and elevation). Then the spatial distribution of MGCs was analyzed at city, cluster, and region scales. Results showed that the relationships between $PM_{2.5}$ and the different factors varied with location. SO_2 emission positively affected $PM_{2.5}$, and the impact was the strongest in the Beijing–Tianjin–Hebei (BTH) region. The impact of NO_2 was generally smaller than that of SO_2 and could be important in coastal areas. The impact of meteorological factors on $PM_{2.5}$ was complicated in terms of spatial variations, with relative humidity and lifted index exerting a strong positive impact on $PM_{2.5}$ in Pearl River Delta and Central China, respectively. Woodland percentage mainly influenced $PM_{2.5}$ in regions of or near deserts, and elevation was important in BTH and Sichuan. The findings of this study can improve our understanding of haze formation and provide useful information for policy-making.

1. Introduction

In recent decades, fine particulate matter or $PM_{2.5}$ (particles with aerodynamic diameters less than 2.5) pollution has become a pressing problem in China (Cheng et al., 2016; Ho et al., 2018a; Ho et al., 2018b; Yang et al., 2019). As a by-product of urbanization and a natural phenomenon, $PM_{2.5}$ can be influenced by many factors, such as anthropogenic emissions, meteorology, and topography (Bei et al., 2018; Chen et al., 2017b; Gui et al., 2019; Sun et al., 2016; Wang et al., 2017c; Yang et al., 2018a). Establishing the relationships between surface $PM_{2.5}$ concentration and these influencing factors (IFs) is important. It can enhance our understanding of the formation mechanism of $PM_{2.5}$ pollution, and also can provide suggestions for policy makers and allow them to implement effectual actions for alleviating $PM_{2.5}$ pollution.

The serious $PM_{2.5}$ pollution in China can be attributed to the increase in emissions (especially anthropogenic emissions) and unfavorable dispersion conditions. Most of the studies conducted on the relationship between $PM_{2.5}$ concentration and these two factors have used model simulation and statistical methods (Cai et al., 2017; Chen et al., 2019; Leung et al., 2018; Liu et al., 2018; Miao et al., 2018). Model simulation methods are based on physical connections and can thoroughly explain the interactions between $PM_{2.5}$ and its IFs despite the complex calculations involved. Statistical methods describe the relationship between $PM_{2.5}$ and its IFs with statistical models, such as simple linear regression, multiple linear regression (MLR), Granger causality test (GCT), and

☆ This paper has been recommended for acceptance by Admir Créso Targino.

* Corresponding author. School of Geodesy and Geomatics, Wuhan University, Wuhan, Hubei, 430079, China.
E-mail address: qqyuan@sgg.whu.edu.cn (Q. Yuan).

https://doi.org/10.1016/j.envpol.2020.114257
0269-7491/

GeoDetector method (Chen et al., 2017a; Ding et al., 2019; Yang et al., 2018a; Zhou et al., 2018). Statistical methods usually ignore the detailed process of interactions but have simple calculation processes and can quantitatively reflect relationships. Therefore, statistical methods have been widely used in relationship analysis. For example, Spearman's correlation coefficients and MLR were used in a previous work to analyze the relationships between $PM_{2.5}$ and meteorological factors (Yang et al., 2017a). In another study, Pearson's correlation coefficients were utilized in the systemic analysis of the $PM_{2.5}$–aerosol optical depth relationship (Yang et al., 2018b).

Two key points must be considered when using statistical methods to quantitatively describe the relationship between two factors. The first one is spatiotemporal heterogeneity. China is a vast country with remarkable geographical diversity. Geographical conditions and their interactions with $PM_{2.5}$ concentration differ widely across regions. Hence, spatial variations must be considered. The second key point is the consideration of the interactions among different IFs. $PM_{2.5}$ concentration and its IFs, such as meteorology, topography, and emissions, form an interactive and organic whole. The consideration of IF "B" may affect the quantitative evaluation of the relationship between $PM_{2.5}$ and IF "A". Thus, statistical models that consider the interactions among different IFs, such as MLR and GCT, can provide more information and describe relationships more accurately than models didn't consider interactions.

The geographically weighted regression (GWR) model was proposed in 1996 and used to explore the relationships among car ownership, social class, and male unemployment (Brunsdon et al., 1996). Since then, the method has been widely used to investigate spatially varying relationships in many fields, including socioeconomics, medicine, and environmental sciences (Gao and Li, 2011; Lin and Wen, 2011; Pineda Jaimes et al., 2010; Wang et al., 2019; Xu and Lin, 2017). GWR can reflect the spatial variations of relationships by building a local regression model at each location (Yang et al., 2017b), and thus can be used to investigate the relationships between $PM_{2.5}$ and its IFs in consideration of the spatial variations and interactions between IFs. However, the problem of implementing this approach is that the coefficients may be biased when the relationships are measured quantitatively. The input variables are usually normalized or standardized only at the global scale, but the coefficients are calculated in each local regression (local scale); hence, the coefficients in different locations are incomparable.

In this study, we added local standardization into the traditional GWR model and proposed the modified GWR coefficients (MGCs) to solve the problem mentioned above. The MGCs were used to investigate the spatially varying relationships between $PM_{2.5}$ concentration and its IFs (including emission and diffusion conditions) in China. In terms of emission-related IFs, we considered sulfur dioxide (SO_2) and nitrogen dioxide (NO_2) emissions, which were approximately represented by SO_2 and NO_2 concentrations respectively in this study. With regard to the IFs about diffusion conditions, we mainly considered the topography and meteorology. Experiments were conducted using 2015 data covering 368 cities and 9 urban agglomerations in China. First, Pearson's correlation coefficients between $PM_{2.5}$ and 24 variables were calculated, and six variables were selected to build the GWR model. Second, the MGCs of the selected variables in different locations were calculated, and the dominant IFs for $PM_{2.5}$ concentration in the different locations were analyzed. Third, an ISODATA clustering experiment was conducted to summarize the main IFs in different cases. Lastly, we analyzed the nine national urban agglomerations in China to describe the dominant IFs for $PM_{2.5}$ pollution at the regional scale. This systemic analysis of the IFs of $PM_{2.5}$ can help in further understanding the $PM_{2.5}$ pollution situation and provide useful information for policy makers.

The rest of this paper is organized as follows. Section 2 is the data and methods part, where we introduce the study area, the data sources, the data preprocessing work, and the methodology. The results and analysis are provided in Section 3. Finally, we make a discussion and summarize our work in Section 4.

2. Data and methods

2.1. Study domain

In 2015, more than 1400 environmental monitoring stations had been established in 368 Chinese cites (Fig. 1(a)). These cities were selected as the study objects in this work. Moreover, urban agglomerations are crucial in promoting the development of regional integration and have thus received considerable attention from the public and government departments. Hence, nine urban agglomerations approved by the National Assembly of China were chosen for our regional-scale research, and their locations are shown in Fig. 1(b). Additional information on the study domain is presented in Supplementary Table 1.

2.2. Data preparation

1) Ground observation data from environmental monitoring stations

Hourly $PM_{2.5}$, SO_2, and NO_2 concentration data for 2015 were provided by the Ministry of Ecology and Environment of the People's Republic of China (http://www.mee.gov.cn/). Simple quality control was applied to the raw data to avoid the impact of outliers. Specifically, consecutive repeats (Rohde and Muller, 2015; Silver et al., 2018) and empty and zero values were eliminated. The hourly data were then averaged to daily data when the number of hours of measurements was not less than 18 (75% coverage of the total 24 h) in a day. The daily data were also averaged to annual data when the number of days of measurements was more than 273 (75% coverage of the total 365 days in 2015) at a particular ground station for subsequent calculation.

2) Topography data

The topographical factors considered in this study were elevation, normalized difference vegetation index (NDVI), and land cover.

Elevation data were obtained from the global multi-data fused seamless DEM product (GSDEM-30). GSDEM-30 is a seamless 30 m DEM dataset that merges SRTM-1, ASTER GDEM v2, and ICESat laser altimetry data, and previous studies have shown that it exhibits good accuracy in China (Yue et al., 2015; Yue et al., 2017). The DEM data were also used to calculate certain terrain indices, including the terrain ruggedness index (TRI), topographic position index (TPI), and roughness (ROUGH). The calculation methods for these indices are provided in the supplementary material (Supplementary Text 1). The GSDEM-30 product can be downloaded from http://sendimage.whu.edu.cn/res/DEM_share/.

NDVI data were obtained from the MODIS NDVI product (MOD13), which was downloaded from the Level 1 and Atmosphere Archive and Distribution System website (https://ladsweb.modaps.eosdis.nasa.gov/search/). Monthly NDVI data at a spatial resolution of 500 m were downloaded and averaged to obtain the annual NDVI.

The land cover data were from the European Space Agency (ESA) Climate Change Initiative (CCI) land cover product, which was downloaded from http://maps.elie.ucl.ac.be/CCI/viewer/index.php.

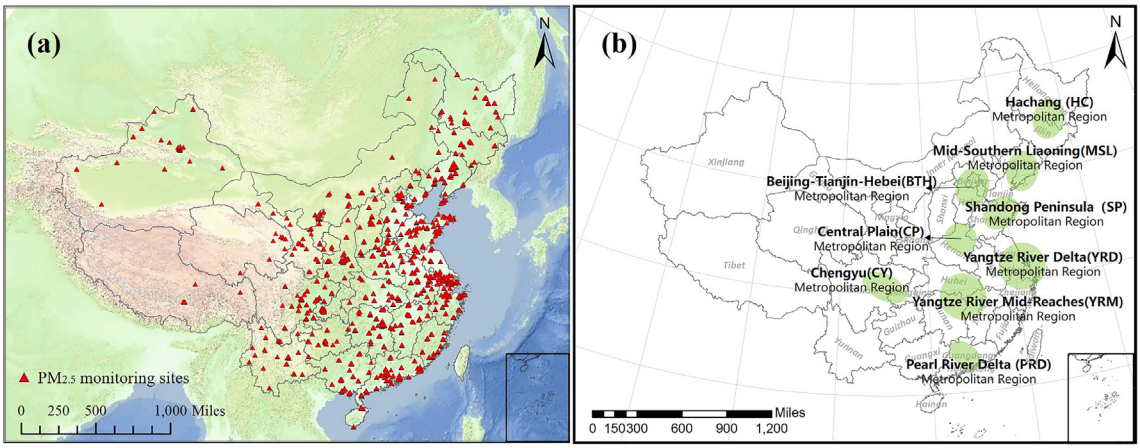

Fig. 1. Study domain. (a) Distribution of $PM_{2.5}$ monitoring sites in 2015. (b) Nine urban agglomerations investigated in this study.

Annual global land cover maps at a spatial resolution of 300 m are published on this website. Land cover in this product is classified into 22 classes, but we integrated these into eight classes in our study for calculation convenience. The eight classes were farmland, woodland, grassland, sparse vegetation, bare land, urban area, water body, and snow and ice. The land cover map for China in 2015 is shown in Supplementary Fig. 1.

3) Meteorological data

The meteorological factors considered in this study were temperature (TMP), pressure (PS), relative humidity (RH), zonal wind speed (UWS), meridional wind speed (VWS), lifted index (LI), vertical speed (VS), precipitation (PR), and planetary boundary layer height (PBLH). The first eight meteorological factors were obtained from the NCEP/NCAR Reanalysis 1 project (https://www.esrl.noaa.gov/psd/data/gridded/data.ncep.reanalysis.surface.html). The spatial resolution of the data is 2.5° × 2.5°, and the temporal resolution is daily. PBLH data were obtained from the MERRA-2 dataset with a spatial resolution of 0.5° × 2/3° and daily temporal resolution (https://disc.gsfc.nasa.gov/datasets/M2T1NXFLX_V5.12.4). Daily meteorological factors were averaged to annual value to match the temporal resolution of topographical data.

A summary of data used in this study was displayed in Table 1.

4) Data integration

The raster products used in this study had various projections and resolutions. When matching these raster products with ground station measurements, these raster products with a projected coordinate system (mainly topographical data) were initially reprojected to the geographic coordinate system of the World Geodetic System 1984 (WGS84) and subsequently resampled to a resolution of 0.1° × 0.1°. Afterward, we used the longitude and latitude information to calculate the corresponding pixels of the ground sites, and the values of the corresponding pixels were matched with those of the ground site measurements. For land cover data, we determined the corresponding pixel of a ground site and calculated the proportion of each type in the 0.1° × 0.1° (= 33 pixels × 33 pixels) rectangular buffer centered at this pixel (Chen et al., 2018; Meng et al., 2016). After these steps, the raster products with different projections and resolutions were matched with the ground station measurements and used for correlation calculation and GWR regression.

2.3. Methodology

Traditional statistical models, such as MLR, usually learn a fixed relationship for different locations and ignore the fact that these relationships can vary with location. Meanwhile, GWR incorporates spatial heterogeneity into the regression model through building a spatially varying relationship between the studied variables (Chen et al., 2016; Sheng et al., 2017). The GWR model can be defined as:

$$y_j = \beta_0(u_j, v_j) + \sum_{i=1}^{p} \beta_i(u_j, v_j)\chi_{ij} + \varepsilon_j$$

where (u_j, v_j) stands for the coordinates for location j, $\beta_i(u_j, v_j)$ refers to the local regression coefficient of the independent variable χ_i at location j, $\beta_0(u_j, v_j)$ represents the intercept, and ε_j is the error term. In this study, we concentrated on the regression coefficients of the different independent variables. Hence, the intercept and error term were ignored. The regression coefficients of the *j*th location are usually estimated using the spatial weighting function. The Gaussian function was used in our study, and it is expressed as:

$$w_{ij} = \exp(-d_{ij}^2 \,/\, b^2)$$

where b is the bandwidth and d_{ij} is the distance between the *i*th and *j*th locations. The optimal bandwidth was determined using the cross-validation method.

Statistically, if all independent and dependent variables have been standardized, then the coefficients of the different variables and locations will be comparable, and a positive and large coefficient will represent a positive and strong impact and vice versa (Vittinghoff et al., 2005; Schroeder et al., 1986). However, in the GWR model, the variables used in each local regression are not strictly standardized. Thus, we modified the coefficients by adding local standardization as follows:

$$\chi_j' = (\chi_j - \mu(\chi_j))/\sigma(\chi_j)$$

$$y_j' = (y_j - \mu(y_j))\,/\,\sigma(y_j)$$

where χ_j' and y_j' are the standardized independent and dependent variables in location j, respectively; $\mu(\chi_j)$ and $\mu(y_j)$ are the mean values of χ_j and y_j, respectively; $\sigma(x_j)$ and $\sigma(y_j)$ are the standard deviations of χ_j and y_j, respectively. After this procedure, we obtained standardized regression coefficients $\beta_0'(u_j, v_j)$ and $\beta_i'(u_j, v_j)$,

Table 1
Variables considered in this study.

Factor	Variable	Abbreviation	Spatial resolution	Data source
Emission	Sulfur dioxide	SO_2	Site-based	Environmental monitoring stations
	Nitrogen dioxide	NO_2	Site-based	Environmental monitoring stations
Meteorology	Temperature	TMP	2.5° × 2.5°	NCEP/NCAR
	Precipitation	PR	2.5° × 2.5°	NCEP/NCAR
	Lifted index	LI	2.5° × 2.5°	NCEP/NCAR
	Meridional wind speed	UWS	2.5° × 2.5°	NCEP/NCAR
	Zonal wind speed	VWS	2.5° × 2.5°	NCEP/NCAR
	Air pressure	PS	2.5° × 2.5°	NCEP/NCAR
	Vertical speed	VS	2.5° × 2.5°	NCEP/NCAR
	Relative humidity	RH	2.5° × 2.5°	NCEP/NCAR
	Planetary boundary layer height	PBLH	0.5° × 0.667°	MERRA-2
Topography	Land cover type	LC1P-LC8P	300 m	ESA CCI land cover
	Farmland percentage	LC1P	300 m	ESA CCI land cover
	Woodland percentage	LC2P	300 m	ESA CCI land cover
	Grassland percentage	LC3P	300 m	ESA CCI land cover
	Sparse vegetation percentage	LC4P	300 m	ESA CCI land cover
	Bare land percentage	LC5P	300 m	ESA CCI land cover
	Urban area percentage	LC6P	300 m	ESA CCI land cover
	Water body percentage	LC7P	300 m	ESA CCI land cover
	Permanent snow and ice percentage	LC8P	300 m	ESA CCI land cover
	Altitude	DEM	30 m	GSDEM-30
	Vegetation index	NDVI	500 m	MODIS
	Terrain ruggedness index	TRI	30 m	Calculated from DEM
	Topographic position index	TPI	30 m	Calculated from DEM
	Roughness	ROUGH	30 m	Calculated from DEM

which are comparable in different locations. We defined the standardized regression coefficients as modified GWR coefficients (MGCs). The MGCs were used in our experiments to explore the relationships between $PM_{2.5}$ and its IFs.

Multicollinearity commonly occurs when many types of independent variables are included in the model, and it could make the GWR model fail or degrade model performance. To avoid this problem, we manually selected the variables through the following steps. First, Pearson's correlation coefficients were calculated between $PM_{2.5}$ concentration and its IFs, and variables with correlation coefficients larger than 0.3 (Jiang et al., 2017) and p-values no more than 0.05 were selected. Second, the variance inflation factors (VIFs) of the selected variables were calculated as follows:

$$VIF(x_i) = \frac{1}{(1 - {R_i}^2)}$$

where $x_i (i = 1, 2 \ldots\ldots, n)$ represents the investigated factors and n is the number of investigated factors. ${R_i}^2$ represents the determination coefficient of the regression equation:

$$x_i = a_1 x_1 + \ldots\ldots + a_{i-1} x_{i-1} + a_{i+1} x_{i+1} + \ldots\ldots + a_n x_n + b$$

Variables with VIFs larger than 10 were excluded (Lin and Wen, 2011). Lastly, the six variables (RH, LI, LC2P, DEM, SO_2, and NO_2) were selected and used as independent variables for the modified GWR model.

3. Results

3.1. Correlation analysis

The Pearson's correlation coefficients between $PM_{2.5}$ concentration and SO_2 and NO_2 emissions, meteorological factors, and topographical variables are listed in Table 2. SO_2 concentration correlated best with $PM_{2.5}$ concentration, followed by LI and NO_2. The correlation of emission factors was generally higher than that of meteorological factors, and the topographical factors showed the lowest correlation. LI, which had been rarely considered in previous $PM_{2.5}$ studies, showed a strong positive correlation with $PM_{2.5}$, with r reaching 0.52. A large LI means the atmosphere is stable and unfavorable for the vertical dispersion of pollutants; when LI is small, the atmosphere is usually unstable, and the strong convection contributes to the diffusion of pollutants, thus reducing the $PM_{2.5}$ concentration (Yang et al., 2017a). The strong positive correlation between $PM_{2.5}$ and LI indicates that vertical atmospheric conditions play a crucial role in $PM_{2.5}$ pollution and deserve further attention. RH, LC2P (woodland percentage), and DEM (elevation) were also highly correlated with $PM_{2.5}$, with the absolute value of r being larger than 0.3. The correlation of PS, VS, PR, LC1P (farmland percentage), TRI, and ROUGH with $PM_{2.5}$ was moderate ($0.2 < r < 0.3$).

Table 2
Correlation coefficients between $PM_{2.5}$ and multiple IFs.

Variable	r	p-value	Variable	r	p-value
Emission			**Diffusion_topography**		
SO_2	0.66	0.00	LC1P	0.29	0.00
NO_2	0.49	0.00	LC2P	−0.33	0.00
			LC3P	0.02	0.40
Diffusion_meteorology			LC4P	−0.10	0.00
TMP	−0.09	0.00	LC5P	0.03	0.25
PS	0.28	0.00	LC6P	0.18	0.00
RH	−0.34	0.00	LC7P	−0.06	0.02
UWS	−0.02	0.56	LC8P	−0.09	0.00
VWS	−0.05	0.05	DEM	−0.32	0.00
LI	0.52	0.00	NDVI	−0.06	0.02
VS	0.21	0.00	TRI	−0.27	0.00
PR	−0.23	0.00	TPI	−0.05	0.09
PBLH	−0.18	0.00	ROUGH	−0.27	0.00

3.2. Coefficient distribution for individual variables

Six variables (SO_2, NO_2, RH, LI, LC2P, and DEM) were selected by using Pearson's correlation coefficients and VIFs as the criteria. Therefore, the GWR model used in our study can be written as:

The distribution of the MGCs for the six variables is shown in Fig. 2. Compared with the normal GWR model, the modified GWR model makes the results in different locations comparable and thus it is more accurate in describing spatial heterogeneity. Overall, SO_2 emission and meteorological conditions exerted a considerable impact on $PM_{2.5}$, whereas the impact of NO_2 emission and topography was weak. However, the impact of these factors also varied significantly with locations, showing strong spatial heterogeneity.

Specifically, the MGCs for SO_2 and NO_2 were positive, which is understandable. SO_2 and NO_2 are the main precursors of secondary particles, which are important components of $PM_{2.5}$ (Xie et al., 2015; Liu et al., 2016). Therefore, high emission levels of SO_2 and NO_2 may benefit the formation of $PM_{2.5}$. In this study, the MGCs of SO_2 were generally larger than that of NO_2 and were the largest among the six variables. This finding implies that SO_2 emission had the most significant influence on $PM_{2.5}$. Furthermore, the MGCs of SO_2 in the Hebei–Henan region, northeastern China, and Sichuan and Guilin Provinces were higher compared with other regions in China, indicating that the same amount of SO_2 emission could lead to a larger increase in $PM_{2.5}$ concentration in these regions than that in other regions. We believe that the large amount of coal combustion and the characteristics of the local environment may be favorable for the transformation of gaseous SO_2 into sulfate, which is a main component of $PM_{2.5}$, thus making the MGC of SO_2 high in these regions (Li et al., 2017a). The MGCs of NO_2 were higher in coastal areas, such as the Shandong Peninsula and several cities

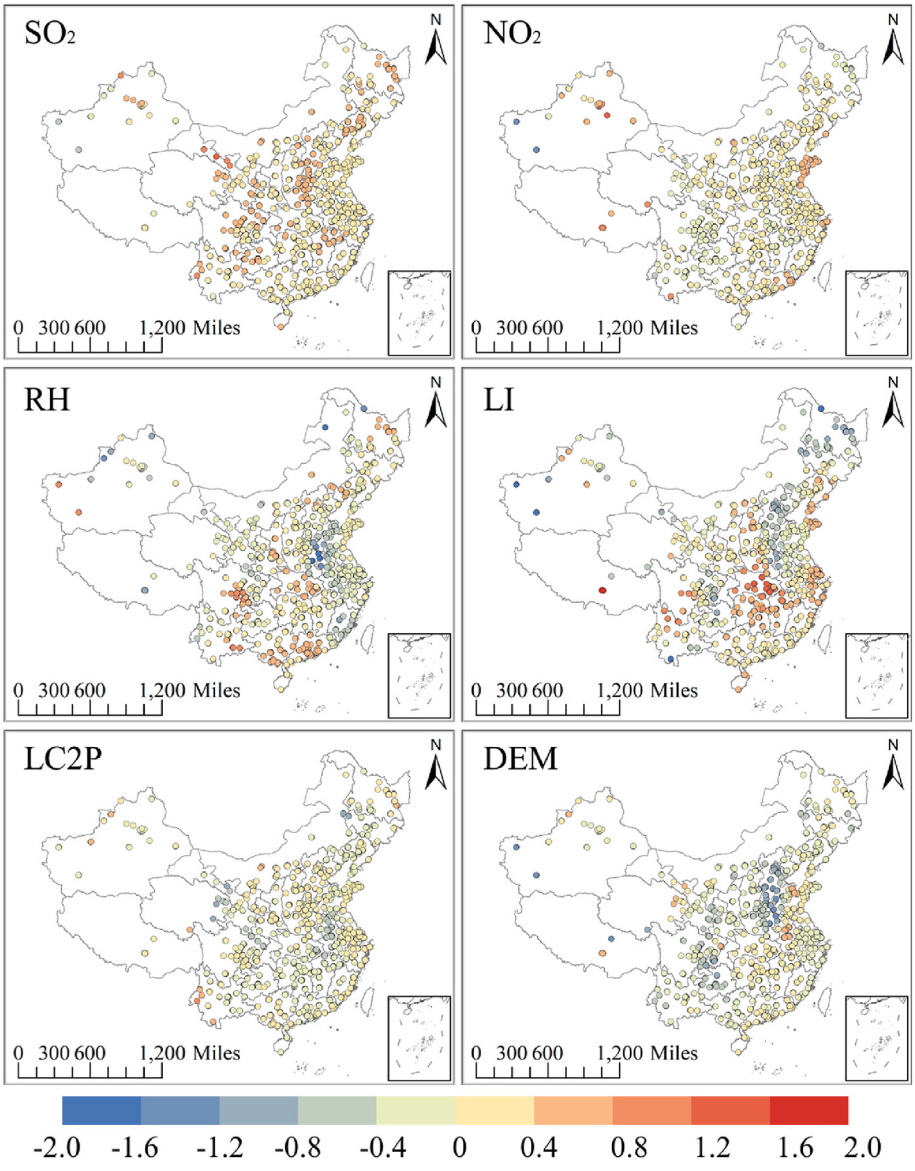

Fig. 2. Distribution of the MGCs of the six variables.

in the Yangtze River Delta (YRD) and Pearl River Delta (PRD) regions. Previous studies have shown that ozone pollution in these coastal regions can be severe (Wang et al., 2017b). The high concentration of ozone combined with high humidity may contribute to the transition from NO_x to nitrate (Wang et al., 2017b; Xu et al., 2019), thereby making the correlation between $PM_{2.5}$ and NO_2 higher than that in other regions.

The distribution of the MGCs for meteorological factors was more complicated than that for emission factors. Specifically, RH had a negative impact on $PM_{2.5}$ in cities on the southeastern side of the Beijing–Tianjin–Hebei (BTH) region. This result suggests that water vapor can exert a wet deposition effect on particles when pollutants are transported from the BTH region to the southeastern YRD region (Fu et al., 2010; Wang et al., 2013). By contrast, the impact of RH was positive in southwestern Sichuan and the PRD region, which means that moisture in the air can promote the formation of particles in these locations (Yang et al., 2017a). The strong impact of LI on $PM_{2.5}$ in central China and its most serious effect in Hubei Province imply that vertical diffusion can be an effective approach for the dilution of $PM_{2.5}$ in this region. According to previous studies, the strong impact of LI on $PM_{2.5}$ in central China may be a result of meteorology–topography interactions (Han et al., 2018; Wang et al., 2017c). The high elevation in northwestern China and the low elevation in southeastern China block the horizontal transportation in central China. The vertical motion thus plays an important role in the formation of good atmospheric circulation, which is favorable for the diffusion of pollutants. Unlike the situation in central China, LI had a negative impact on $PM_{2.5}$ in the BTH region, namely, the $PM_{2.5}$ concentration is low when LI is high (the atmosphere is stable).

The MGCs for the topographical factors were smaller than those for the meteorological factors. The impact of woodland percentage (LC2P) on $PM_{2.5}$ concentration was weak, with most of the MGCs falling between −0.35 and 0.3. However, the small negative MGCs (with a large absolute value) for northwestern Gansu and Qinghai Province imply a relatively strong negative impact of woodland cover on $PM_{2.5}$ pollution. Many deserts are located in or around northwestern Gansu and Qinghai Province. Therefore, dust storms could be the main source of air pollutants (Ta et al., 2004). Tree planting in these regions can reduce desertification and $PM_{2.5}$ concentration. Hence, woodland coverage has a larger negative impact on $PM_{2.5}$ in these regions than in other regions of China. Meanwhile, the MGCs of DEM (elevation) were mainly negative in the BTH area. Several researchers have demonstrated that Yan Mountains in the north and Taihang Mountains in the west can trap pollutants from the south (which has a lower elevation than the northern region) and stop the transport to the northern BTH region (which has a higher elevation than the southern region) (Yang et al., 2016; Zhang et al., 2013). These conditions may result in a negative relationship between $PM_{2.5}$ and DEM. Furthermore, the MGCs of DEM for the Chengyu region were also negative. This result is consistent with the pollution situation in Sichuan Province, which has serious pollution in Sichuan Basin (low elevation) and low pollution in West Sichuan Plateau (high elevation) (Li et al., 2017b; Li et al., 2017c; Shen et al., 2018). This finding agrees with that of a previous study, which reported that topography has a large impact on $PM_{2.5}$ in Sichuan Province (Yang et al., 2018b).

The map shown in Fig. 3 illustrates the distribution of the main IFs in different locations. For a certain location, we can acquire the MGCs for the six factors included in the regression model. The factor with the largest absolute value of MGC was regarded as the main IF of $PM_{2.5}$ in this location. The legend shows the varying symbols representing the different factors.

$$PM_{2.5,j} = \beta_1'(u_j, v_j)SO_{2,j} + \beta_2'(u_j, v_j)NO_{2,j} + \beta_3'(u_j, v_j)RH_j + \beta_4'(u_j, v_j)LI_j + \beta_5'(u_j, v_j)LC2P_j + \beta_6'(u_j, v_j)DEM_j$$

3.3. Cluster analysis

On the basis of the MGCs of the six variables, we classified the cities into several types by using the ISODATA clustering algorithm (Anderberg, 2014). A detailed explanation of the clustering method is presented in the supplementary material. The MGCs clustering results and boxplots of the MGCs of different clusters are displayed in Fig. 4. Six types were clustered in total. The first type is mainly composed of Hebei, Henan, southern Gansu, and the southwestern part of Sichuan Basin. The MGCs of the cities in this cluster were not very high, and the impact of SO_2 and DEM on $PM_{2.5}$ was relatively large. The cities in the second type are mainly located in central China and include Hubei, Hunan, and Jiangxi Provinces. The most notable feature of this cluster is the strong impact of LI on $PM_{2.5}$. The MGCs of LI in the cities belonging to this type ranged from 0.26 to 1.83 with an average value of 0.84, which far outweighed the MGCs of LI in the other cities. The third type of cities is concentrated in the BTH region. The $PM_{2.5}$ concentration in the cities belonging to this type was largely influenced by DEM, followed by SO_2 emission. As for the fourth type of cities, the distribution of the included cities is discrete. This type is typically made up of cities in Heilongjiang Province, northern Hebei, and southwestern Sichuan Basin and SO_2 is the dominant IF of $PM_{2.5}$. The cities in the fifth cluster are mainly located on the southern side of the BTH region and form a band from Shandong to Fujian. RH is the most important IF of $PM_{2.5}$ in this “city band”. The appearance of this cluster is interesting because of its consistency with the blue region in the MGCs distribution map of RH in Fig. 2. The pollution feature of this “city band” could be a future research topic. The last type is composed of cities in the Shandong Peninsula, YRD, and PRD regions, all of which are in the southeastern coastal areas of China. The MGCs of this type of cities were close to zero, and the absolute values did not exceed 0.5. This result indicates that $PM_{2.5}$ concentration in these cities was not considerably affected by the six variables studied in our research compared with cities of the other types. On the one hand, this minimal influence may be due to the relatively weak pollution in these coastal regions. On the other hand, several factors that were ignored in this research, such as solar radiation and temperature, could have a large impact on $PM_{2.5}$ in coastal regions (N. Galindo et al., 2007; Glavasa et al., 2008).

3.4. Analysis of typical regions

The analysis results for the nine national urban agglomerations are shown in Fig. 5. Overall, the impact of SO_2 emission on $PM_{2.5}$ was stable, positive, and the most uniform while the impact of the other variables varied in the different urban agglomerations.

Apart from sulfate and nitrogen emissions, $PM_{2.5}$ in the BTH

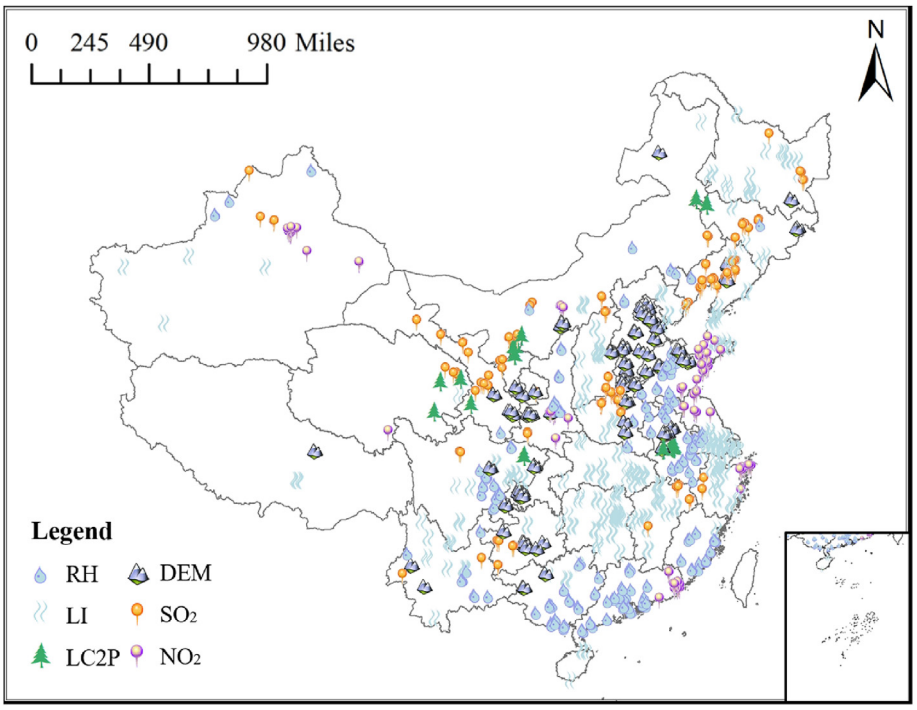

Fig. 3. Main IFs of $PM_{2.5}$ in different locations. The main IFs are determined using the MGC values.

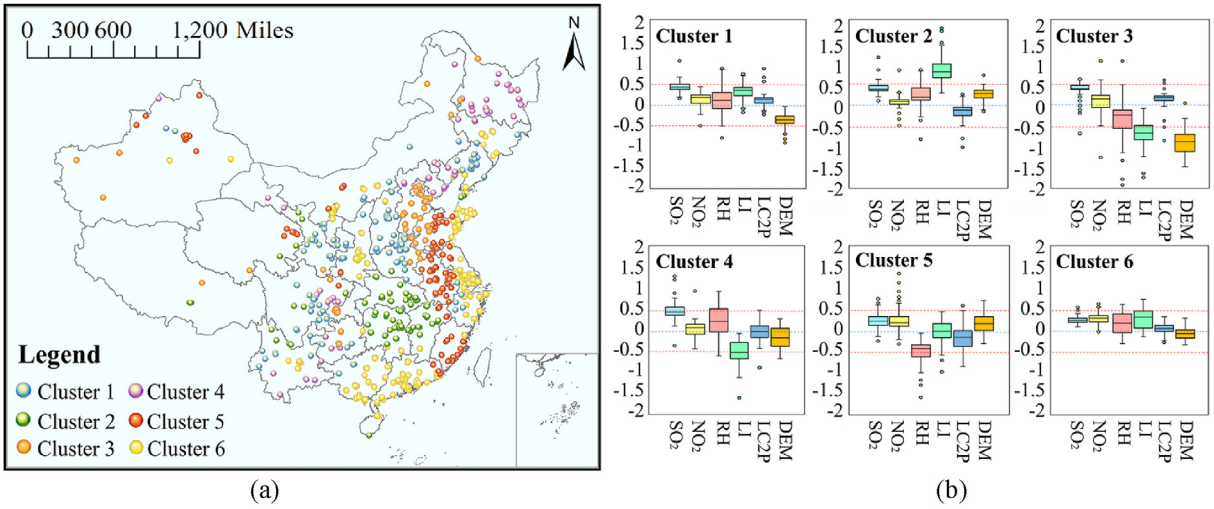

Fig. 4. (a) Clustering results according to the MGCs of the six variables using the ISODATA method (the different colors represent the different cluster types) and (b) boxplots of the MGCs of the six clusters. Each color represents the MGCs of one variable. The upper and bottom borders of the box denote the upper and lower quartiles, respectively, and the line in the middle of the box refers to the median value. The max and min values are marked with dashes, and the anomalous values are presented by circles. (For interpretation of the references to color in this figure legend, the reader is referred to the Web version of this article.)

region is also considerably influenced by DEM. A high DEM value is usually accompanied by low $PM_{2.5}$ concentration. The high mountains in the BTH region may have trapped the pollutants in the low-elevation areas and caused serious pollution in the low-elevation areas (Zhang et al., 2016; Yang et al., 2016). RH was the dominant IF of $PM_{2.5}$ concentration in the PRD region. A high RH value can help increase $PM_{2.5}$ concentrations. For the Central Plain and Chengyu regions, SO_2 and DEM were the two most important IFs of $PM_{2.5}$ concentration. The positive impact of SO_2 and the negative impact of DEM imply that the SO_2 emission and blocking effect of high mountains may be the two most important reasons for air pollution in the Central Plain and Chengyu regions. The greatest impact of LI on $PM_{2.5}$ in the mid-reaches of the Yangtze River demonstrates that the $PM_{2.5}$ pollution in this region is dominated by meteorological factors, and the impact of emissions and topography is weak. The $PM_{2.5}$ concentrations in YRD, Shandong Peninsula, mid-southern Liaoning, and Hachang regions were not significantly affected by the six variables compared with those in the other urban agglomerations; all of the absolute values of MGCs were not larger than 0.4. Specifically, in the YRD region, the impact of SO_2 on $PM_{2.5}$ was the smallest among all the urban agglomerations. Previous studies have shown that the contribution of regional transport to $PM_{2.5}$ pollution accounts for a larger percentage than the contribution of local emissions in the YRD region.

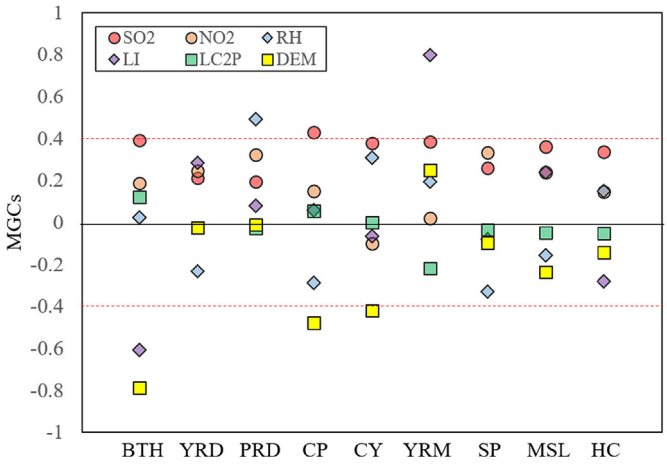

Fig. 5. MGCs of SO_2, NO_2, RH, LI, LC2P, and DEM for the nine urban agglomerations. The MGCs of the urban agglomerations are averaged by using the MGCs of the cities in the urban agglomerations. The nine agglomerations are denoted by their abbreviations: BTH for Beijing-Tianjin-Hebei, YRD for Yangtze River Delta, PRD for Pearl River Delta, CP for Central Plain, CY for Chengyu region, YRM for Yangtze River Mid-Reaches area, SP for Shandong Peninsula, MSL for Mid-Southern Liaoning, and HC for Hachang urban agglomeration.

For example, regional transport accounts for 54%, 50%, and 48% of the $PM_{2.5}$ pollution in Shanghai, Jiangsu, and Zhejiang, respectively, which altogether occupy a large area in the YRD region (Xue et al., 2014). Therefore, the drivers of regional transport-based pollution, such as horizontal wind speed, may be important factors of $PM_{2.5}$ pollution in the YRD region (Yang et al., 2017a). Meanwhile, SO_2 was the dominant IF in mid-southern Liaoning and Hachang regions, which are located in northeastern China. This finding is consistent with that of a previous study, which showed that sulfate is the dominant fraction of $PM_{2.5}$ in northeastern China because of industrial and domestic coal combustion (Ying et al., 2014); hence, the MGCs of SO_2 are high. The high MGCs of SO_2 in the BTH and Central Plain regions can be attributed to the same reason.

4. Discussion and conclusions

4.1. Temporal variations

As mentioned in the Introduction, spatial and temporal variations are important when conducting a relationship analysis. However, we did not analyze the temporal variations in the experiments due to the limited access to sufficient multitemporal land cover data. Nevertheless, realizing the importance of examining temporal variations (especially inter-annual variations), we discussed the inter-annual variations of the MGCs through a less-strict experiment. Given that we only had access to land cover data in 2013, 2014, and 2015 and other data ranging from 2013 to 2017, we assumed that land cover remained the same after 2015 to ensure that the 2015 land cover data represented those in 2016 and 2017. For each year from 2013 to 2017, we calculated the correlation between $PM_{2.5}$ and the 24 variables mentioned previously, and the variables with correlations larger than 0.3 and VIF values less than 10 were used to build the GWR model. SO_2 and NO_2 were highly correlated with $PM_{2.5}$ in all the years. Therefore, we calculated the inter-annual variation rate of the MGCs of SO_2 and NO_2. The varying rate was represented by the slope of the linear regression and the results are shown in Fig. 6. The left side of the figure shows that the MGCs of SO_2 for Henan, South Hebei, Sichuan, Liaoning, and Jilin decreased over time, indicating the weakening impact of SO_2 emission on $PM_{2.5}$. This result may be due to the environmental protection policies implemented in these regions. However, the increasing MGCs of SO_2 in the PRD region demonstrate that additional attention must be paid to SO_2 emission in this region. The MGCs of NO_2 also increased over time in Hebei, Beijing, and Shaanxi. A comparison of SO_2 and NO_2 MGC variations showed that the pollution control policies at present may be more effective in SO_2 control than in NO_2 control.

4.2. Limitations and future work

Although MGCs can improve the comparability of coefficients in different locations, this indicator is merely a relative variable. For

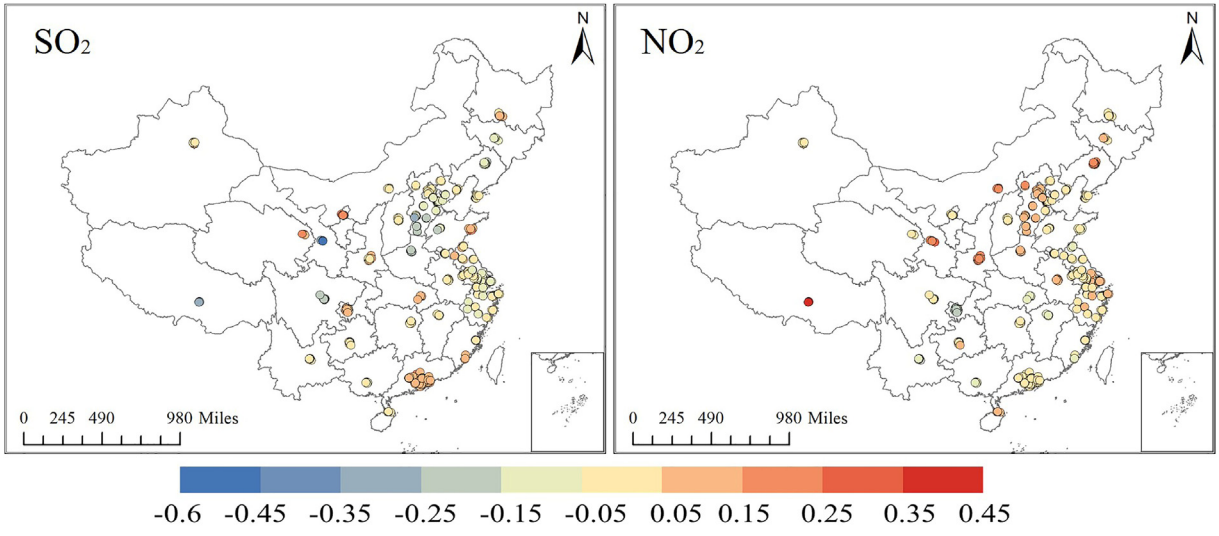

Fig. 6. Inter-annual variations in the MGCs of SO_2 and NO_2 from 2013 to 2017. The color of the point corresponds to the slope of the linear regression, which was fitted using data from 2013 to 2017 at each point and represented the inter-annual varying rate. (For interpretation of the references to color in this figure legend, the reader is referred to the Web version of this article.)

example, if the MGC of DEM is 2, then a 1 m increase in DEM will not necessarily lead to a 2 $\mu g/m^3$ increase in $PM_{2.5}$. MGC is only meaningful for comparisons. If the MGC of DEM and RH is 2 and 4, respectively, then RH influences $PM_{2.5}$ more than DEM does. Therefore, if we wish to acquire the absolute impact of these IFs on $PM_{2.5}$ concentration, then MGC may be a poor indicator. This feature also increases the sensitivity of the MGC results to variable selection in the sense that different variable selections can lead to different results.

Furthermore, some results in this study could not be fully explained and further investigation is needed. For example, the reasons for the negative MGCs of LI in the BTH region and the high NO_2 MGCs in the coastal regions remain unclear. Further research with physical models may be necessary to compensate for the limitations of statistical models, such as the disregard of the physical mechanism.

In this study, we used SO_2 and NO_2 data to represent the emission factors. Although these data are highly correlated with sulfate and nitrogen emissions, certain disadvantages still exist. First, SO_2 and NO_2 can have similar sources to $PM_{2.5}$. Sharing sources can induce the high correlation between the variables and possibly lead to large regression coefficients, which may mislead our understanding and interpretation of the results to a certain degree. Although SO_2 and NO_2 in this study were mainly regarded as emission indicators and the probability of misunderstanding is small, replacing SO_2 and NO_2 with real emission factors is still preferable. Second, sulfate and nitrogen are not the only emission sources. Several other emission factors ignored in our study may limit the generalizability of our results. In the future, we will consider using an emission inventory to represent the emission amount and thus improve the accuracy and interpretability of the model.

Lastly, the validation of the proposed modified GWR model can be an interesting research direction. Several state-of-the-art statistical models for detecting the relationships between multiple factors, such as GeoDetector (Wang and Xu, 2017a), may be used for a systematic comparison, and meanwhile, serve as a validation for the proposed method.

4.3. Conclusions

We analyzed the relationships between $PM_{2.5}$ concentration and emissions, topography, and meteorology in China by using a newly proposed indicator called MGC. This method can accurately capture the spatial variations in the impact of different factors and some interesting results were obtained in this study. First, SO_2 and NO_2 emissions exerted a positive effect on the $PM_{2.5}$ concentration in most regions. SO_2 dominated the $PM_{2.5}$ pollution in regions with high domestic and industrial coal combustion, such as Hebei and Henan, and NO_2 was important in coastal regions, such as the Shandong Peninsula. Second, the impact of meteorological factors significantly varied with location. RH had a strong influence on $PM_{2.5}$ in the city band on the southern side of the BTH region, and LI was the most dominant factor of $PM_{2.5}$ pollution in Central China. Lastly, the impact of topography was weaker than that of meteorology. LC2P only influenced $PM_{2.5}$ largely in regions with serious desertification, such as northern Gansu. DEM exerted a large impact on $PM_{2.5}$ in the BTH region and Sichuan Province. The proposed MGC considers the spatial heterogeneity and interactions while being comparable in different locations, and exhibited satisfactory performance in investigating the relationship between $PM_{2.5}$ and numerous IFs. The results of our experiments can offer instructive information in the process of formulating pollution-control policies in the different regions to ensure that the policies are suitable for local situations.

CRediT authorship contribution statement

Qianqian Yang: Data curation, Methodology, Formal analysis, Writing - original draft. **Qiangqiang Yuan:** Conceptualization, Supervision, Writing - review & editing, Formal analysis. **Linwei Yue:** Resources, Supervision, Writing - review & editing. **Tongwen Li:** Resources, Methodology, Writing - review & editing.

Acknowledgments

We gratefully acknowledge the support from the Strategic Priority Research Program of the Chinese Academy of Sciences (No. XDA19090104), the National Natural Science Foundation of China (No. 41922008), the Science and Technology Major Project of Hubei Province (No. 2019AAA046), and the Fundamental Research Funds for the Central Universities of Wuhan Univeristy (No. 2042019kf0213). The authors would also like to thank the China National Environmental Monitoring Center for providing the $PM_{2.5}$ data. The MODIS NDVI data were obtained from the Atmospheric Science Data Center of NASA Langley Research Center. The NCEP/NCAR reanalysis data were sourced from NOAA/OAR/ESRL PSD. The MERRA-2 data were acquired from NASA GES DISC. Lastly, the authors express their gratitude to the land cover product team of ESA/CCI for providing the land cover data.

Appendix A. Supplementary data

Supplementary data to this article can be found online at https://doi.org/10.1016/j.envpol.2020.114257.

References

Anderberg, M.R., 2014. Cluster Analysis for Applications: Probability and Mathematical Statistics: A Series of Monographs and Textbooks, 19. Academic Press.
Bei, N., Zhao, L., Wu, J., Li, X., Feng, T., Li, G., 2018. Impacts of sea-land and mountain-valley circulations on the air pollution in Beijing-Tianjin-Hebei (BTH): a case study. Environ. Pollut. 234, 429–438.
Brunsdon, C., Fotheringham, A.S., Charlton, M.E., 1996. Geographically Weighted Regression: A Method for Exploring Spatial Nonstationarity. Geographical Analysis 28 (4), 281–298.
Cai, W., Li, K., Liao, H., Wang, H., Wu, L., 2017. Weather conditions conducive to Beijing severe haze more frequent under climate change. Nat. Clim. Change 7, 257–262.
Chen, Q., Mei, K., Dahlgren, R.A., Wang, T., Gong, J., Zhang, M., 2016. Impacts of land use and population density on seasonal surface water quality using a modified geographically weighted regression. Sci. Total Environ. 572, 450–466.
Chen, Z., Cai, J., Gao, B., Xu, B., Dai, S., He, B., Xie, X., 2017a. Detecting the causality influence of individual meteorological factors on local PM2.5 concentration in the Jing-Jin-Ji region. Sci. Rep. 7, 40735.
Chen, Z., Xie, X., Cai, J., Chen, D., Gao, B., He, B., Cheng, N., Xu, B., 2017b. Understanding meteorological influences on PM2.5 concentrations across China: a temporal and spatial perspective. Atmos. Chem. Phys. Discuss. 1–30.
Chen, L., Gao, S., Zhang, H., Sun, Y., Ma, Z., Vedal, S., Mao, J., Bai, Z., 2018. Spatio-temporal modeling of PM2.5 concentrations at the national scale combining land use regression and Bayesian maximum entropy in China. Environ. Int. 116, 300–307.
Chen, S., Guo, J., Song, L., Li, J., Liu, L., Cohen, J.B., 2019. Inter-annual variation of the spring haze pollution over the North China Plain: roles of atmospheric circulation and sea surface temperature. Int. J. Climatol. 39, 783–798.
Cheng, Z., Luo, L., Wang, S., Wang, Y., Sharma, S., Shimadera, H., Wang, X., Bressi, M., de Miranda, R.M., Jiang, J., Zhou, W., Fajardo, O., Yan, N., Hao, J., 2016. Status and characteristics of ambient PM2.5 pollution in global megacities. Environ. Int. 89–90, 212–221.
Ding, Y., Zhang, M., Qian, X., Li, C., Chen, S., Wang, W., 2019. Using the geographical detector technique to explore the impact of socioeconomic factors on PM2.5 concentrations in China. J. Clean. Prod. 211, 1480–1490.
Fu, Q., Zhuang, G., Li, J., Huang, K., Wang, Q., Zhang, R., Fu, J., Lu, T., Chen, M., Wang, Q., Chen, Y., Xu, C., Hou, B., 2010. Source, long-range transport, and characteristics of a heavy dust pollution event in Shanghai. J. Geophys. Res. 115.
Galindo, N., Nicolás, J.F., Yubero, E., Caballro, S., Pastor, C., Crespo, J., 2007. Factors affecting levels of aerosol sulfate and nitrate on the Western Mediterranean coast. Atmos. Res. 88, 305–313.
Gao, J., Li, S., 2011. Detecting spatially non-stationary and scale-dependent relationships between urban landscape fragmentation and related factors using Geographically Weighted Regression. Appl. Geogr. 31, 292–302.

Glavas, Sotirios.D., Nikolakis, Panayiotis, Ambatzoglou, Demetrios, Mihalopoulos, Nikos, 2008. Factors affecting the seasonal variation of mass and ionic composition of PM2.5 at a central Mediterranean coastal site. Atmos. Environ. 42, 5365–5373.

Gui, K., Che, H., Wang, Y., Wang, H., Zhang, L., Zhao, H., Zheng, Y., Sun, T., Zhang, X., 2019. Satellite-derived PM2.5 concentration trends over Eastern China from 1998 to 2016: relationships to emissions and meteorological parameters. Environ. Pollut. 247, 1125–1133.

Han, S., Hao, T., Zhang, Y., Liu, J., Li, P., Cai, Z., Zhang, M., Wang, Q., Zhang, H., 2018. Vertical observation and analysis on rapid formation and evolutionary mechanisms of a prolonged haze episode over central-eastern China. Sci. Total Environ. 616, 135–146.

Ho, H.C., Wong, M.S., Yang, L., Chan, T.C., Bilal, M., 2018a. Influences of socioeconomic vulnerability and intra-urban air pollution exposure on short-term mortality during extreme dust events. Environ. Pollut. 235, 155–162.

Ho, H.C., Wong, M.S., Yang, L., Shi, W., Yang, J., Bilal, M., Chan, T.C., 2018b. Spatiotemporal influence of temperature, air quality, and urban environment on cause-specific mortality during hazy days. Environ. Int. 112, 10–22.

Jiang, M., Sun, W., Yang, G., Zhang, D., 2017. Modelling seasonal GWR of daily $PM_{2.5}$ with proper auxiliary variables for the Yangtze River Delta. Rem. Sens. 9 (4), 346.

Leung, D.M., Tai, A.P.K., Mickley, L.J., Moch, J.M., van Donkelaar, A., Shen, L., Martin, R.V., 2018. Synoptic meteorological modes of variability for fine particulate matter (PM2.5) air quality in major metropolitan regions of China. Atmos. Chem. Phys. 18, 6733–6748.

Li, H., Zhang, Q., Zhang, Q., Chen, C., Wang, L., Wei, Z., Zhou, S., Parworth, C., Zheng, B., Canonaco, F., Prévôt, A.S.H., Chen, P., Zhang, H., Wallington, T.J., He, K., 2017a. Wintertime aerosol chemistry and haze evolution in an extremely polluted city of the North China Plain: significant contribution from coal and biomass combustion. Atmos. Chem. Phys. 17, 4751–4768.

Li, T., Shen, H., Yuan, Q., Zhang, X., Zhang, L., 2017b. Estimating ground-level PM2.5 by fusing satellite and station observations: a geo-intelligent deep learning approach. Geophys. Res. Lett. 44 (11), 985-911,993.

Li, T., Shen, H., Zeng, C., Yuan, Q., Zhang, L., 2017c. Point-surface fusion of station measurements and satellite observations for mapping PM 2.5 distribution in China: methods and assessment. Atmos. Environ. 152, 477–489.

Lin, C.-H., Wen, T.-H., 2011. Using geographically weighted regression (GWR) to explore spatial varying relationships of immature mosquitoes and human densities with the incidence of dengue. Int. J. Environ. Res. Publ. Health 8, 2798–2815.

Liu, T., Wang, X., Hu, Q., Deng, W., Zhang, Y., Ding, X., et al., 2016. Formation of secondary aerosols from gasoline vehicle exhaust when mixing with SO_2. Atmos. Chem. Phys. 16 (2), 675–689.

Liu, Q., Wang, S., Zhang, W., Li, J., Dong, G., 2018. The effect of natural and anthropogenic factors on PM2.5: empirical evidence from Chinese cities with different income levels. Sci. Total Environ. 653, 157–167.

Meng, X., Fu, Q., Ma, Z., Chen, L., Zou, B., Zhang, Y., Xue, W., Wang, J., Wang, D., Kan, H., Liu, Y., 2016. Estimating ground-level PM(10) in a Chinese city by combining satellite data, meteorological information and a land use regression model. Environ. Pollut. 208, 177–184.

Miao, Y., Liu, S., Guo, J., Huang, S., Yan, Y., Lou, M., 2018. Unraveling the relationships between boundary layer height and PM2.5 pollution in China based on four-year radiosonde measurements. Environ. Pollut. 243, 1186–1195.

Pineda Jaimes, N.B., Bosque Sendra, J., Gómez Delgado, M., Franco Plata, R., 2010. Exploring the driving forces behind deforestation in the state of Mexico (Mexico) using geographically weighted regression. Appl. Geogr. 30, 576–591.

Rohde, R.A., Muller, R.A., 2015. Air pollution in China: map- ping of concentrations and sources. PloS One 10, e0135749. https://doi.org/10.1371/journal.pone.0135749.

Schroeder, Larry D., Sjoquist, David L., Stephan, P.E., 1986. Understanding Regression Analysis. Sage Publications, pp. 31–32.

Shen, H., Li, T., Yuan, Q., Zhang, L., 2018. Estimating regional ground-level PM2.5 directly from satellite top-of-atmosphere reflectance using deep belief networks. J. Geophys. Res.: Atmosphere 123 (24), 13875–13886.

Sheng, J., Han, X., Zhou, H., 2017. Spatially varying patterns of afforestation/reforestation and socio-economic factors in China: a geographically weighted regression approach. J. Clean. Prod. 153, 362–371.

Silver, B., Reddington, C.L., Arnold, S.R., Spracklen, D.V., 2018. Substantial changes in air pollution across China during 2015–2017. Environ. Res. Lett. 13, 114012. https://doi.org/10.1088/1748-9326/aae718.

Sun, L., Wei, J., Duan, D.H., Guo, Y.M., Yang, D.X., Jia, C., Mi, X.T., 2016. Impact of Land-Use and Land-Cover Change on urban air quality in representative cities of China. J. Atmos. Sol. Terr. Phys. 142, 43–54.

Ta, W., Xiao, H., Qu, J., Xiao, Z., Yang, G., Wang, T., Zhang, X., 2004. Measurements of dust deposition in Gansu Province, China, 1986–2000. Geomorphology 57, 41–51.

Vittinghoff, Eric, Glidden, David V., Shiboski, Stephen C., McCulloch, C.E., 2005. Regression Methods in Biostatistics: Linear, Logistic, Survival, and Repeated Measures Models. Springer, pp. 75–76.

Wang, J.F., Xu, C.D., 2017a. Geodetector: principle and prospective. Acta Geograph. Sin. 72 (1), 116–134.

Wang, X., Dickinson, R.E., Su, L., Zhou, C., Wang, K., 2017c. PM2.5 Pollution in China and How it Has Been Exacerbated by Terrain and Meteorological Conditions. Bulletin of the American Meteorological Society.

Wang, L., Du, H., Chen, J., Zhang, M., Huang, X., Tan, H., Kong, L., Geng, F., 2013. Consecutive transport of anthropogenic air masses and dust storm plume: two case events at Shanghai, China. Atmos. Res. 127, 22–33.

Wang, T., Xue, L., Brimblecombe, P., Lam, Y.F., Li, L., Zhang, L., 2017b. Ozone pollution in China: a review of concentrations, meteorological influences, chemical precursors, and effects. Sci. Total Environ. 575, 1582–1596.

Wang, J., Wang, S., Li, S., 2019. Examining the spatially varying effects of factors on PM2.5 concentrations in Chinese cities using geographically weighted regression modeling. Environ. Pollut. 248, 792–803.

Xie, Y., Zhao, B., Zhang, L., Luo, R., 2015. Spatiotemporal variations of PM2.5 and PM10 concentrations between 31 Chinese cities and their relationships with SO_2, NO_2, CO and O_3. Particuology 20, 141–149.

Xu, B., Lin, B., 2017. Factors affecting CO2 emissions in China's agriculture sector: evidence from geographically weighted regression model. Energy Pol. 104, 404–414.

Xu, J., Zhu, F., Wang, S., Zhao, X., Zhang, M., Ge, X., Wang, J., Tian, W., Wang, L., Yang, L., Ding, L., Lu, X., Chen, X., Zheng, Y., Guo, Z., 2019. Impacts of relative humidity on fine aerosol properties via environmental wind tunnel experiments. Atmos. Environ. 206, 21–29.

Xue, W., Fu, Fei, Wang, Jinnan, Tang, Guiqian, Lei, Yu, Yang, Jintian, Wang, Y., 2014. Numerical study on the characteristics of regional transport of PM2.5 in China. China Environ. Sci. 36, 2353–2360.

Yang, H., Chen, J., Wen, J., Tian, H., Liu, X., 2016. Composition and sources of PM2.5 around the heating periods of 2013 and 2014 in Beijing: implications for efficient mitigation measures. Atmos. Environ. 124, 378–386.

Yang, Q., Yuan, Q., Li, T., Shen, H., Zhang, L., 2017a. The relationships between PM2.5 and meteorological factors in China: seasonal and regional variations. Int. J. Environ. Res. Publ. Health 14, 1510–1528.

Yang, X., Wang, S., Zhang, W., Zhan, D., Li, J., 2017b. The impact of anthropogenic emissions and meteorological conditions on the spatial variation of ambient SO2 concentrations: a panel study of 113 Chinese cities. Sci. Total Environ. 584–585, 318–328.

Yang, D., Wang, X., Xu, J., Xu, C., Lu, D., Ye, C., Wang, Z., Bai, L., 2018a. Quantifying the influence of natural and socioeconomic factors and their interactive impact on PM2.5 pollution in China. Environ. Pollut. 241, 475–483.

Yang, Q., Yuan, Q., Yue, L., Li, T., Shen, H., Zhang, L., 2018b. The relationships between PM2.5 and AOD in China: about and behind spatiotemporal variations. Environ. Pollut. 248, 526–535.

Yang, Y., Li, J., Zhu, G., Yuan, Q., 2019. Spatio-temporal relationship and evolvement of socioeconomic factors and PM2.5 in China during 1998-2016. Int. J. Environ. Res. Publ. Health 16.

Ying, Q., Wu, L., Zhang, H., 2014. Local and inter-regional contributions to PM2.5 nitrate and sulfate in China. Atmos. Environ. 94, 582–592.

Yue, L., Shen, H., Yuan, Q., Zhang, L., 2015. Fusion of multi-scale DEMs using a regularized super-resolution method. Int. J. Geogr. Inf. Sci. 29, 2095–2120.

Yue, L., Shen, H., Zhang, L., Zheng, X., Zhang, F., Yuan, Q., 2017. High-quality seamless DEM generation blending SRTM-1, ASTER GDEM v2 and ICESat/GLAS observations. ISPRS J. Photogrammetry Remote Sens. 123, 20–34.

Zhang, A., Qi, Q., Jiang, L., Zhou, F., Wang, J., 2013. Population exposure to PM2.5 in the urban area of beijing. PloS One 8, e63486.

Zhang, H., Wang, Z., Zhang, W., 2016. Exploring spatiotemporal patterns of PM2.5 in China based on ground-level observations for 190 cities. Environ. Pollut. 216, 559–567.

Zhou, C., Chen, J., Wang, S., 2018. Examining the effects of socioeconomic development on fine particulate matter (PM2.5) in China's cities using spatial regression and the geographical detector technique. Sci. Total Environ. 619–620, 436–445.